Nor Mohd Haziq Norsahperi
Senior Lecturer
Universiti Putra Malaysia
Department of Electrical and Electronics Engineering, Faculty of Engineering, 43400, UPM Serdang, Malaysia

Salmiah Ahmad
Associate Professor
International Islamic University Malaysia
Department of Mechanical Engineering, Kulliyah of Engineering, 53100, Gombak, Malaysia

Siti Fauziah Toha
Associate Professor
International Islamic University Malaysia
Department of Mechatronics Engineering, Kulliyah of Engineering, 53100, Gombak, Malaysia

Mohd Azri Abd Mutalib
Engineer
SIRIM Berhad
Machine Design Section, Machinery Technology Centre, No. 1A, Persiaran Zurah, Kawasan Perindustrian Rasa, 44200, Hulu Selangor, Malaysia

Design, Simulation and Experiment of PSO-FOPID Controller for Height Position Control of a Scissor Mechanism Platform

This paper proposes the PSO-FOPID controller, which is a Fractional Order Proportional-Integral-Derivative (FOPID) controller tuned using particle swarm optimization with spreading factor algorithm for height position control of a scissor mechanism platform. The tuning process of five control gains in the FOPID controller is technically challenging to achieve high position accuracy. In this study, this problem is addressed through the offline tuning method by using particle swarm optimization with the spreading factor algorithm to reduce the complexity in tuning the control gains. From the experimental study, it is found that the proposed controller can eliminate the steady-state error under the two input references with approximately 1.5% and 0.9% reductions of the overshoot and undershoot in the height position response as compared to its promising performances in simulations. It is envisaged that the PSO-FOPID controller can be useful in designing effective height position control of a non-linear platform.

Keywords: *Motorised Adjustable Vertical Platform, Fractional Order PID, Particle Swarm Optimisation, Scissor Mechanism, Satellite Test, Optimal Control*

1. INTRODUCTION

Satellite is essential for a wide range of communication technologies, and it has been extensively used for climate and environmental monitoring [1,2]. Before launching satellites into geostationary orbit, the satellites should undergo various tests, especially thermal tests, as illustrated in Figure 1, to examine the survivability of the satellites at an extreme temperature, as mentioned in [3,4]. As most of the satellite tests are commonly conducted in a clean room, one of the greatest challenges is to lift heavy satellites in such confined space. To address this challenge, the scissor mechanism is employed in a satellite handling platform system known as the motorized adjustable vertical platform (MAVeP) such that the satellite can be lifted safely during its operations [5]. Nevertheless, reliable control for the scissor mechanism is necessarily required to control the movement of the scissor mechanism platform.

Although various modern control strategies have been developed and studied for various application domains, the proportional-integral-derivative (PID) controller is of interest because of its simplicity and practicality. Several researchers have reported that the PID controller has been implemented in approximately 90% of the systems in numerousindustries [6-9]. Des–pite its long history in the control engineering field, the PID controller has several problems in use as it becomes less effective in the non-linear and uncertain system [10, 11]. Because of this shortcoming, several attempts have been made to improve the capability of the PID controller. As a result, the fractional-order PID (FOPID) controller has been introduced, where two additional non-integer orders in the derivative and integral terms are added in the control algorithm to increase the flexibility, robustness, and stability of the PID controller [12-14].

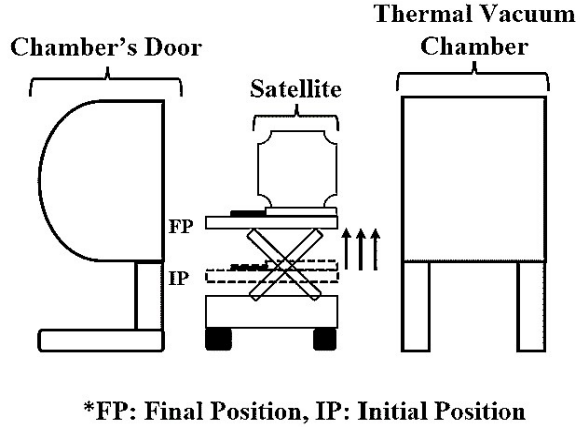

Figure 1. Scissor mechanism platform operation

Existing research recognizes the critical role played by the FOPID controller where a wide range of practical applications has been embedded with the FOPID controller, such as robotics [15, 16], aerodynamic system [9, 17], and automatic voltage regulator [18]. However, the determination of the five gains in the FOPID control algorithm to ensure the FOPID controller can produce the desired system performance

Received: August 2021, Accepted: December 2021
Correspondence to: Dr Nor Mohd Haziq Norsahperi
Faculty of Engineering,
Universiti Putra, PM Serdang, Malaysia
E-mail: nmhaziq@upm.edu.my
doi:10.5937/fme2201046N

is technically challenging. Various tuning techniques have been introduced to identify the five gains in the FOPID control algorithm, such as Ziegler-Nichols, Astrom-Hagglund, and frequency-based analyses [4, 11, 19, 20]. However, these classical tuning techniques necessitate an exact dynamic model and in-depth knowledge of the system, which are not always available and do not always represent the non-linear system dynamics. Although the study in [4] has evaluated the effectiveness of the FOPID controller in the scissor mechanism platform through simulations using the Ziegler-Nichols and Astrom-Hagglund methods, these classical theoretical-based tuning methods are cumbersome and require complex analyses in the frequency domain. Moreover, the promising results in [4] are validated through simulations without experimental evidence.

Numerous studies have attempted to employ artificial intelligence techniques to determine the five gains in the FOPID control algorithm, such as ant colony optimization [11], particle swarm optimization (PSO), neural network [9], genetic algorithm [21], and cuckoo search algorithm [22]. Although various optimization algorithms have emerged, the PSO algorithm is of particular interest since it has several attractive features, including fewer parameters, low computational cost, and fast convergence [23–25]. Several attempts have been made to further improve the performance of the PSO algorithm. As a result, particle swarm optimization (PSO) with spreading factor (PSO-SF) algorithm was developed to avoid the algorithm being trapped in local optima[9, 26].

Therefore, this paper proposes the PSO-FOPID controller, which is the FOPID controller tuned using the particle swarm optimization (PSO) with spreading factor (PSO-SF) algorithm for height position control of the scissor mechanism platform. In contrast to the existing study in [4], the proposed control design does not require a precise dynamic model in the frequency domain or extensive system knowledge. Furthermore, to the best of the authors' knowledge, this study is the first implementation of the proposed controller to the scissor mechanism platform. Consequentially, the main contributions of this study are highlighted as follows:

- Development of the PSO-FOPID controller to attain the optimal five gains of the FOPID controller using the PSO-SF algorithm for the scissor mechanism platform application and avoid the cumbersome theoretical-based method.
- The viability of the proposed PSO-FOPID controller is experimentally validated using the laboratory scissor mechanism platform, considering the step and time-varying input references.

This paper has been organized in the following way. This paper begins by giving a brief overview of the FOPID controller and then, it moves on to describe the proposed PSO-FOPID controller design. The third section is concerned with the experimental setup, whereas the fourth section represents all simulation and experiment results, including a discussion of the findings. The final section then summarises the main findings of this study.

2. PSO-FOPID CONTROL DESIGN

In contrast to the classical PID controller, the FOPID control has two additional non-integer orders in the derivative and integral terms where it can be described in the s-domain as:

$$U(s)_{FOPID} = K_P E(s) + K_i \frac{E(s)}{S^{\lambda}} + K_d s^{\mu} E(s) \quad (1)$$

where $U(s)_{FOPID}$ is the control signal of the FOPID controller, the error, $e(t)$ between the desired height position response, $y_d(t)$, and the height position response of the system, $y_a(t)$ is given by $e(t) = y_d(t) - y_a(t)$; and $E(s)$ denotes the error, $e(t)$ in the s-domain. The proportional, integral, and derivative gains are represented by K_p, K_i, and K_d, respectively, like the classical PID controller. Besides, λ and μ represent the non-integer orders in the integral and derivative terms, respectively. The closed-loop system with the FOPID controller can be depicted as shown in Figure 2.

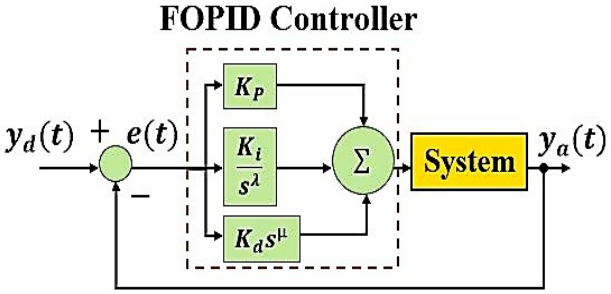

Figure 2. A closed-loop system with the FOPID controller

Although the FOPID controller has increased the flexibility, robustness, and stability region of the classical PID controller, the offline tuning process of the five gains in the FOPID controller in (1) using the theoretical-based methods to achieve the high position accuracy is a challenging task. To address this issue, the PSO-SF algorithm is adopted for offline tuning all five gains of the FOPID controller in (2) such that high position accuracy can be achieved. This proposed controller is called the PSO-FOPID controller throughout this paper.

Similar to the conventional PSO algorithm, the PSO-SF algorithm starts by randomly distributing a group of particles around the search space. In every iteration, the movement of each particle, n, to search for the minimum value of the fitness function is based on the best individual position, p_b, the best position in the population, G_b, the position, p^i_n, and the velocity, v^i_n of the current epoch, i. The searching process by the particles will always carry on until the maximum number of the epoch, i_{max} is accomplished. The new position p_n^{i+1} can be determined by:

$$p_n^{i+1} = p_n^i + v_n^{i+1} \quad (2)$$

$$v_n^{i+1} = \omega v_n^i + \delta_1 R\left(p_{bn}^{\ i} - p_n^i\right) + \delta_2 R\left(G_{bn}^{\ i} - p_n^i\right) \quad (3)$$

where v_n^{i+1} is the new velocity, ω denotes the inertia weight, R is the random number within the range of [0,1], while δ_1 and δ_2 represent acceleration coefficients.

In contrast to the conventional PSO algorithm, the values of the ω, δ_1, and δ_2 parameters are varying in every epoch to avoid being trapped in local optima with fast convergence to the minimum fitness value, as mentioned by [9, 26]. The value of the ω, δ_1, and δ_2 parameters can be computed by:

$$\omega = e^{\left(\frac{-i}{s_{pi}{}_{\max}}\right)} \quad (4)$$

$$\delta_1 = \delta_2 = 2\left(1 - \frac{i}{i_{\max}}\right) \quad (5)$$

where edenotes the exponential function and $Sp = 0.5(\varepsilon + \alpha)$ represents the spreading factor with $\varepsilon\alpha$and are the spread and deviation of the particles in the search space, respectively. Overall, the pseudocode of the PSO-FOPID controller can be summarised in Table 1.

Table 1. Pseudocode of the PSO-FOPID controller

1: Initialise the parameters and bounds in the PSO-SF algorithm, such as ω, δ_1, δ_2, i_{max}, *n, p* and *v.* 2: Set the desired minimum value of the selected fitness function to a small number.
3: The particles, *n* are randomly distributed in the search space and within the specified bound.
4: **While** $i \neq i_{max}$
Do
i. Evaluate the values of the particle fitness using the selected fitness function.
ii. **If** the current individual fitness of an individual particle is better than the previous p_b, **then** update the new p_b. **If not,** maintain the previous p_b.
iii. Select the new G_b. **If** the current G_b is better than the previous G_b, **then** update the new G_b. **If not,** maintain the previous G_b.
iv. Compute the new ω, δ_1, and δ_2 using (4-5), respectively.
v. Compute new position, p_n^{i+1} and new velocity, v_n^{i+1} using (2-3), concerning its specified ranges.
5: **End While** ($i = i_{max}$).

The parameters of the PSO-SF algorithm used in the PSO-FOPID control design are summarised in Table 2. Noted that the 3D virtual model of the scissor mechanism platform in [4] is used for the gain tuning process of the PSO-FOPID controller, and the mean square error, *MSE* as in (6) is selected as the fitness function.

$$MSE = \frac{\sum_{k=1}^{N}\left(e(k)\right)^2}{N}, k = 1,...,N \quad (6)$$

where N is the total number of sampling data. The number of swarms inTable 2 is determined by the heuristic method such that the algorithm does not require a high computational cost during the tuning process. As for the number of swarms, the number is selected based on the number of control gains available in the FOPID controller. Besides, the range of acceleration factors and the range of inertia factors are selected based on the authors' explanation in [9, 26]. So far, this paper has described the PSO-FOPID controller design and the next section that follows moves on to describe the experimental setup.

Table 2. PSO-SF parameters for gain tuning of the PSO-FOPID controller

Parameters	Values
Maximum number of epochs, i_{max}	100
Number of swarms	10
Number of particles, n	5
Range of acceleration factors, δ_1 and δ_2	[0.05,2]
Range of inertia factor, ω	[0,1]

3. EXPERIMENTAL SETUP

Experiments are carried out on a laboratory scissor mechanism platform to further validate the simulation findings. Figure 3 represents the laboratory scissor mechanism platform system with an analog distance infrared sensor.

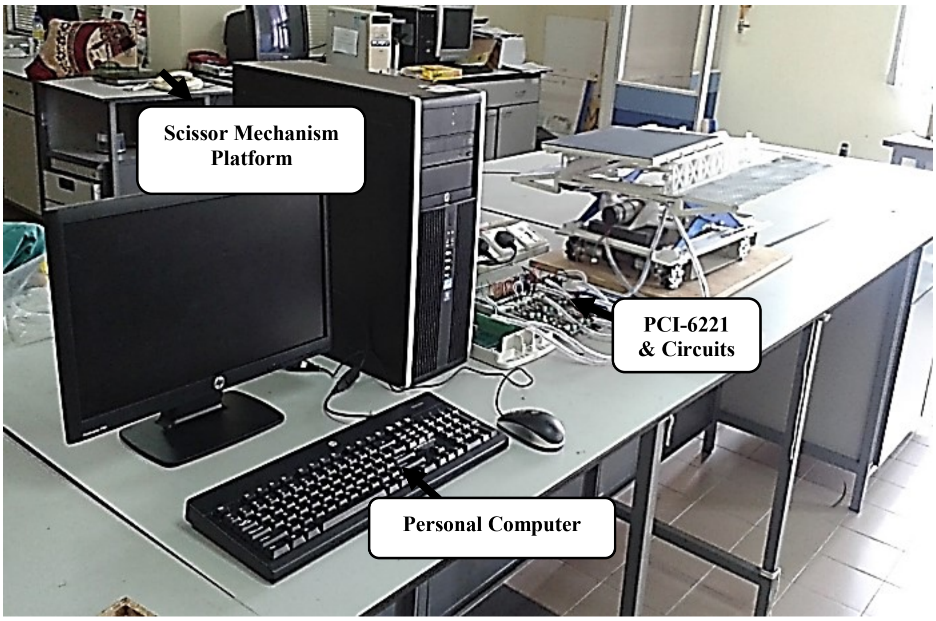

Figure 3. Experimental setup of scissor mechanism platform system

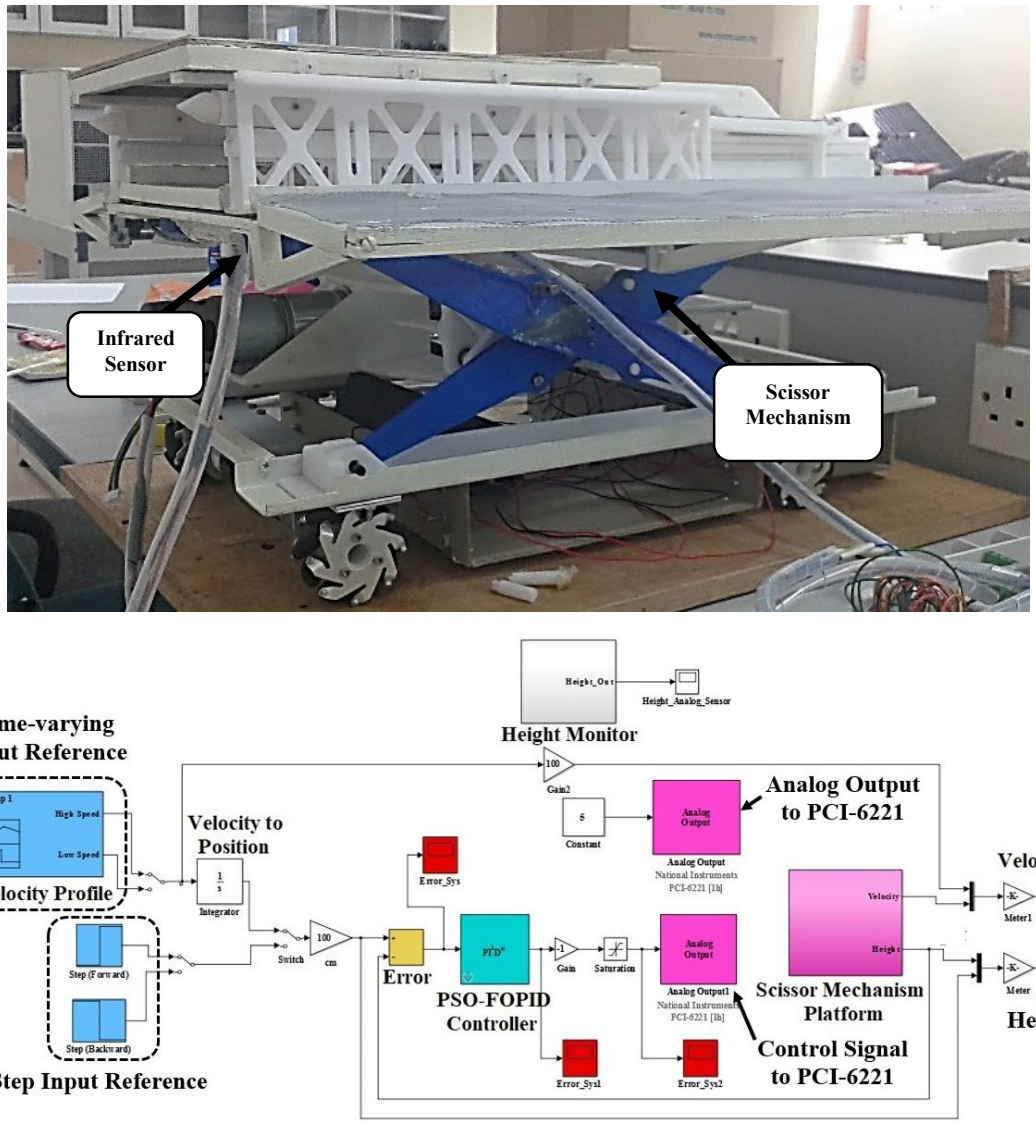

Figure 4. Scissor mechanism platform system: (a) location of the infrared sensor and (b) control system configuration in the Real-Time Window Target application

The height measurement from the infrared sensor in Figure 4. Scissor mechanism platform system: (a) loca–tion of the infrared sensor and (b) control system confi–guration in the Real-Time Window Target appli–cation a) is transferred online to a personal computer via an interface module comprising a NI PCI-6221 and power supply circuits in Figure 3. Besides, the expe–rimental results are extracted by using the Real-Time Window Target application on the MATLAB software, and the control system configuration in the application is illus–trated in Figure 4 (b). In order to build the control system configuration in Figure 4 (b), the Data Acquisition toolbox for the National Instruments devices is used to enable Simulink to recognise the NI PCI-6221 inputs and outputs. This includes the use of the FOMCON toolbox to build the FOPID control algorithm in the Simulink for experiments as well as simulations.

Table 3 presents the scissor mechanism platform system parameters used in the simulations and expe–riments, as stated in [4]. In this section, the experimental setup to validate the viability of the PSO-FOPID cont–roller has been briefly explained. The following section then presents and comprehensively discusses all simu–lation and experiment findings in this study.

Table 3. Scissor mechanism platform parameters [4]

	Descriptions	Values
Structure	Upper Deck (UP) mass	5 kg
	Small Scissor (SS) mass	0.0925 kg
	Main Scissor (MS) mass	1.295 kg
	Ball Screw Clamper (C2) mass	0.957 kg
	Motor Clamper (C1) mass	0.956kg
	DC motor mass	0.36 kg
	Ball Screw Set mass	0.5 kg
	Clamper (C1 and C2) dimension	0.240×0.06×0.07m
	Main Scissor (MS) length	0.3886m
	Small Scissor (SS) length	0.0654m
	Upper Deck (UP) dimension	0.2652×0.595m
DC Motor	Threaded Pitch	0.0015m
	No-load speed	7.0162 rad/s
	Rated load speed	6.5973 rad/s
	Rated power output	41.3 Watt
	DC supply voltage	12 V
	Rotor damping	0.297 N·m/(rad/s)

4. RESULTS AND DISCUSSION

This section presents simulation and experimental findings of the implementation of the proposed PSO-FOPID controller in the scissor mechanism platform. The main aim of this approach is to maintain the height of the scissor mechanism platform at the desired height considering step and time-varying input references. Simulations using the 3D virtual model as shown in [4] and experiments using the laboratory scissor mechanism platform as shown in Section 0 are carried out to assess and validate the performances of the PSO-FOPID controller. The configuration of the scissor mechanism platform with the PSO-FOPID controller is depicted in Figure 5 with the assumption that a sensor model has unity gain. Figure 5 also briefly illustrates the offline tuning process of the PSO-FOPID controller for the simulations and experiments.

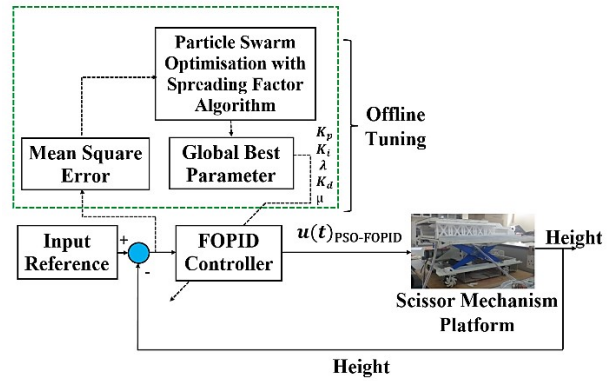

Figure 5. Configuration of the PSO-FOPID controller in a scissor mechanism platform

To evaluate the viability of the proposed PSO-FOPID controller, the following case studies are carried out for simulations and experiments by using MATLAB software:

Case I (Simulation) : Height position response with step input reference.
Case II (Simulation) : Height position response with a square wave signal input reference.
Case III (Experiment) : Height position response with step input reference.
Case IV (Experiment) : Height position response with time-varying input reference.

The sampling period for all case studies is set to 1.0ms, and this study uses two standard criteria to provide a detailed explanation of the performances: 1. height position characteristics and 2. mean square error (*MSE*) in (6). Table 4 presents the selected values of the proposed PSO-FOPID and FOPID controllers. Note that the parameters of the FOPID controller are tuned using Nichols-Ziegler and Astrom-Hagglund techniques as explained in [4].

Table 4. Selected controller parameters

Parameters	FOPID [4]	PSO-FOPID
K_p	4	5.7651
K_i	1.2	6.117
λ	0.7	0.6035
K_d	4.1	5
μ	0.89	0.7827

The convergence profile of the particles to the global minimum of the search space for the PSO-FOPID controller is shown in Figure 6. It is apparent from Figure 6in which the values of the fitness function, *MSE* easily reach the minimum value ($MSE = 8.033 \times 10^{-6}$) at about 90 iterations to attain the optimum values of the five gains of the PSO-FOPID controller.

4.1 Simulation findings

The purpose of Case I (simulation) and Case II (simulation) is to assess the height position responses of the PSO-FOPID controller against the FOPID controller when the scissor mechanism platform is subjected to step and square wave input references. Figure 7 and Table 5 compare the results obtained from the case studies. The findings for the Case I (simulation) study as shown in Figure 7 and Table 5, indicate that there are significant reductions of the overshoot, *PO* and undershoot, *UDP* of the PSO-FOPID controller as compared to the FOPID controller by approximately 0.12% and 0.78%, respectively. Moreover, it is apparent from Table 5 that the rise time, *Tr*, and the settling time, T_s of the PSO-FOPID controller, are about 70% and 52% faster than the FOPID controller, respectively. These findings have important implications for developing a satellite handling platform for a confined space application, where low overshoot and low undershoot in the position responses with fast response are desirable features.

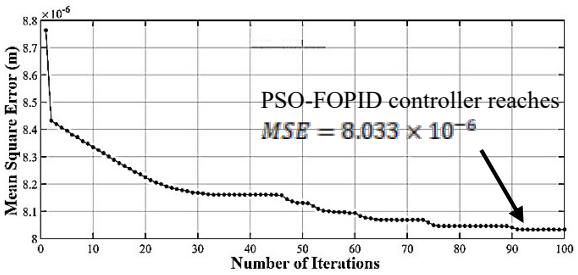

Figure 6. Convergence curve of the fitness function, *MSE*

Although both controllers produce no steady-state error, e_{ss}, the most significant finding is significant reductions in the *MSE* values of the PSO-FOPID controller as compared to the FOPID controller for Case I (simulation) and Case II (simulation) by approximately 50% and 46%, respectively. So far, the PSO-FOPID controller has shown to be able to produce promising performances as compared to the FOPID controller in simulations. Despite these promising results, experiment studies should be undertaken to further evaluate the performance of the PSO-FOPID controller in hardware using the laboratory scissor mechanism platform, and the following section discusses the experimental findings.

Table 5. Simulation height position characteristics of all controllers for Case I (simulation)

Performance	FOPID [4]	PSO-FOPID
$T_r(s)$	1.0284	0.2979
$T_s(s)$	1.8458	0.6849
$PO(\%)$	1.8037	1.6836
$UDP(\%)$	1.7203	0.9386
e_{ss}	0	0

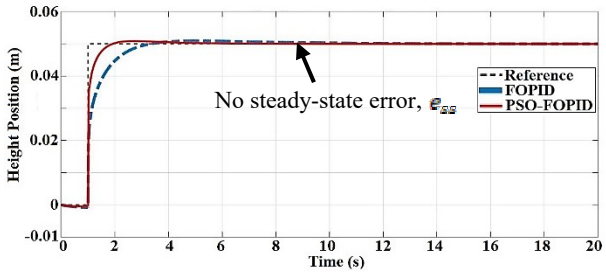

(a)

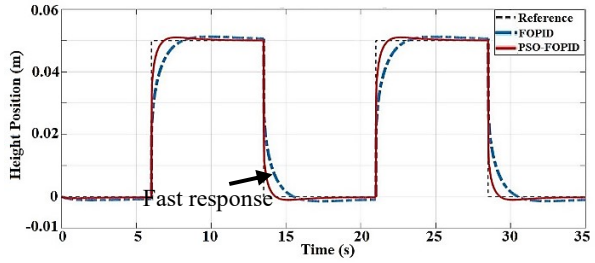

(b)

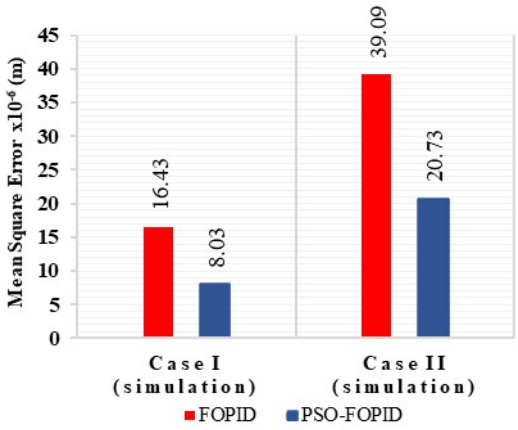

(c)

Figure 7. Height position responses of a simulated scissor mechanism platform for (a) Case I (simulation), (b) Case II (simulation), and (c) mean square error, *MSE*

4.2 Experimental findings

Turning now to the experimental findings on the PSO-FOPID controller where the scissor mechanism platform is set up as in Figure 3 and the experimental results are shown in Figure 8 and Table 6. It is apparent from Table 6 that the superiority of the PSO-FOPID controller is confirmed by about a 1.5% reduction of the overshoot, *PO*, and elimination of the undershoot, *UDP* in the height position responses for Case III (experiment) as compared to the simulation results. Moreover, the most compelling finding is that the PSO-FOPID controller still produces no steady-state error, e_{ss} which is in agreement with the simulation findings. The findings of this experimental study suggest that the PSO-FOPID controller not only can produce a promising performance in simulations but also can reproduce it in the hardware.

Despite these promising results, the PSO-FOPID controller slows down the height position response in terms of the rise time, T_r, and the settling time, T_s as shown in Table 6, which is not consistent with the simulation findings. It seems possible that these results may be due to the mismatch between the hardware and the 3D virtual model, which is inevitable, as mentioned by [27]. Moreover, these results are also likely related to the DC motor in the laboratory scissor mechanism platform reaching its maximum speed. The speed saturation of the DC motor issue may be handled by incorporating an anti-windup compensator into the proposed controller.

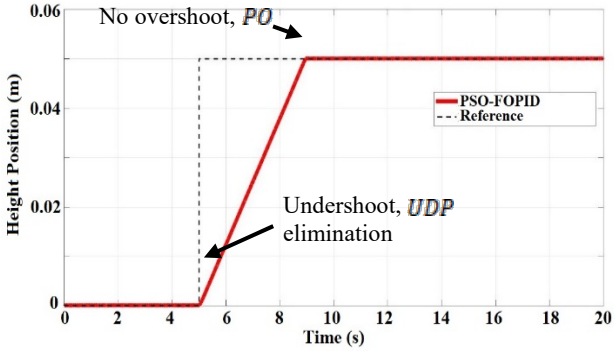

(a)

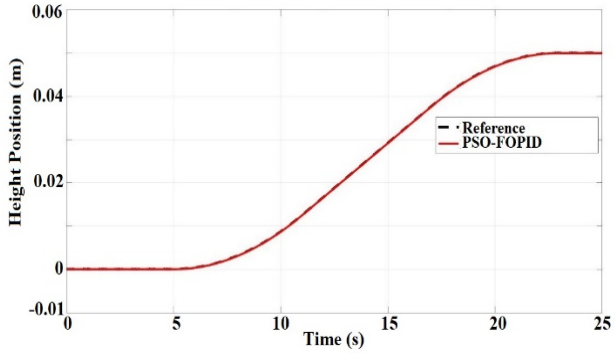

(b)

Figure 8. Height position responses of a laboratory scissor mechanism platform for (a) Case III (experiment) and (b) Case IV (experiment)

Table 6. Experimental height position characteristics of all controllers for Case III (experiment)

Performance	Simulation	Experiment
$T_r(s)$	0.2979	3.1326
$T_s(s)$	0.6849	3.8665
$PO(\%)$	1.6836	0.2565
$UDP(\%)$	0.9386	0
e_{ss}	0	0

5. CONCLUSION

The main goal of the current study is to design the PSO-FOPID controller for the scissor mechanism platform and evaluate the viability of the PSO-FOPID controller through experiments considering the step and time-varying input references. The most critical finding from this study is that the PSO-FOPID controller provides promising performance in terms of the fast responses and high position accuracy compared to the FOPID controller considering the step and time-varying input references in simulations. Moreover, these experiments using the laboratory scissor mechanism platform confirmed that the PSO-FOPID controller also could reproduce almost similar performances in terms of the height position accuracy with zero value of the steady-

state error as in the simulations. The current findings add to a growing body of literature on the practical implementation of the FOPID controller.

As an extension of our work, it would be interesting to consider other uncertainties that may present in the practical implementation, such as external disturbances and parameter variations, such that the capability of the PSO-FOPID controller can be further evaluated. Besides, it is recommended that further research explore the use of the multi-objective PSO algorithm to attain the optimal gains of the FOPID controller so that more criteria, such as the height position accuracy and energy consumption, can be considered concurrently. Moreover, further research might investigate the control efforts of the PSO-FOPID controller to further validate its performances in practical cases.

ACKNOWLEDGEMENT

This project was funded by the Ministry of Science, Technology, and Innovation of Malaysia (MOSTI) through the Malaysia Space Agency (MYSA). This work is a collaboration of Universiti Putra Malaysia (UPM), International Islamic University Malaysia (IIUM), SIRIM Berhad, and MYSA to design and develop the Motorised Adjustable Vertical Platform for the satellite test facilities at AITC in Malaysia.

REFERENCES

[1] Zhou, F. Wang, R. and Bian, J.: Performance analysis of non-orthogonal multiple access based-satellite communication networks with hardware impairments and channel estimations, Electron. Lett., Vol. 56, No. 1, pp. 52–55, 2020.

[2] Xu, L. Abbaszadeh, P. Moradkhani, H. Chen, N. and Zhang, X.: Continental drought monitoring using satellite soil moisture, data assimilation, and an integrated drought index, Remote Sens. Environ., Vol. 250, No. August, pp. 112028, 2020.

[3] Leng, E.W.L. Salleh, N. Salim, H. Sabri, S.F. and Ismail, M.: Design and development of Motorized Adjustable Vertical Platform (MAVeP) for satellite test facility, in: *2015 International Conference on Space Science and Communication (IconSpace)*, pp. 424–427, 2015.

[4] Norsahperi, N.M.H. Ahmad, S. Toha, S.F. Mahmood, I.A. and Hanif, N.H.H.M.: Robustness analysis of fractional-order PID for an electrical aerial platform, J. Mech. Sci. Technol., Vol. 32, No. 11, pp. 5411–5419, 2018.

[5] Norsahperi, N.M.H. Ahmad, S. Toha, S.F. and Mahmood, I.A.: Analysis and practical validation on multi-linkage scissor platforms drive system for the satellite test facilities, Int. J. Heavy Veh. Syst., Vol. 28, No. 1, pp. 1, 2021.

[6] Feyo, A. Thelkar, A. Bharatiraja, C. and Adedayo, Y.: Reference design and comparative analysis of model reference adaptive control for steam turbine speed control, FME Trans., Vol. 48, No. 2, pp. 329–341, 2020.

[7] Åström, K.J. and Hägglund, T.: The future of PID control, Control Eng. Pract., Vol. 9, No. 11, pp. 1163–1175, 2001.

[8] Nie, Z.-Y. Zhu, C. Wang, Q.-G. Gao, Z. Shao, H. and Luo, J.-L.: Design, analysis, and application of a new disturbance rejection PID for uncertain systems, ISA Trans., Vol. 101, pp. 281–294, 2020.

[9] Norsahperi, N.M.H., and Danapalasingam, K.A.: Particle swarm-based and neuro-based FOPID controllers for a Twin Rotor System with improved tracking performance and energy reduction, ISA Trans., Vol. 102, pp. 230–244, 2020.

[10] Ajwad, S.A. Iqbal, J. Islam, R.U. Alsheikhy, A. Almeshal, A. and Mehmood, A.: Optimal and Robust Control of Multi DOF Robotic Manipulator: Design and Hardware Realization, Cybern. Syst., Vol. 49, No. 1, pp. 77–93, 2018.

[11] Mughees, A. and Mohsin, S.A.: Design and Control of Magnetic Levitation System by Optimizing Fractional Order PID Controller Using Ant Colony Optimization Algorithm, IEEE Access, Vol. 8, pp. 116704–116723, 2020.

[12] Tepljakov, A. Alagoz, B.B. Yeroglu, C. Gonzalez, E.A. Hosseinnia, S.H. Petlenkov, E. Ates, A. and Cech, M.: Towards Industrialization of FOPID Controllers: A Survey on Milestones of Fractional-Order Control and Pathways for Future Developments, IEEE Access, Vol. 9, pp. 21016–21042, 2021.

[13] Arya, Y.: A novel CFFOPI-FOPID controller for AGC performance enhancement of single and multi-area electric power systems, ISA Trans., Vol. 100, pp. 126–135, 2020.

[14] Yousaf, S. Mughees, A. Khan, M.G. Amin, A.A. and Adnan, M.: A Comparative Analysis of Various Controller Techniques for Optimal Control of Smart Nano-Grid Using GA and PSO Algorithms, IEEE Access, Vol. 8, pp. 205696–205711, 2020.

[15] Gheisarnejad, M. and Khooban, M.H.: An Intelligent Non-Integer PID Controller-Based Deep Reinforcement Learning: Implementation and Experimental Results, IEEE Trans. Ind. Electron., Vol. 68, No. 4, pp. 3609–3618, 2021.

[16] Huang, H.-C. and Chuang, C.-C.: Artificial Bee Colony Optimization Algorithm Incorporated With Fuzzy Theory for Real-Time Machine Learning Control of Articulated Robotic Manipulators, IEEE Access, Vol. 8, pp. 192481–192492, 2020.

[17] Basu, A. Mohanty, S. and Sharma, R.: Designing of the PID and FOPID controllers using conventional tuning techniques, in: *International Conference on Inventive Computation Technologies (ICICT)*, pp. 1–6 , 2016.

[18] Ayas, M.S. and Sahin, E.: FOPID controller with fractional filter for an automatic voltage regulator, Comput. Electr. Eng., Vol. 90, pp. 106895, 2021.

[19] Azarmi, R. Tavakoli-Kakhki, M. Sedigh, A.K. and Fatehi, A.: Analytical design of fractional order PID controllers based on the fractional set-point weighted structure: Case study in twin rotor

helicopter, Mechatronics, Vol. 31, pp. 222–233, 2015.

[20] Mandić, P.D. Šekara, T.B. Lazarević, M.P. and Bošković, M.: Dominant pole placement with fractional order PID controllers: D-decomposition approach, ISA Trans., Vol. 67, pp. 76–86, 2017.

[21] Devaraj, S.V. Gunasekaran, M. Sundaram, E. Venugopal, M. Chenniappan, S. Almakhles, D.J. Subramaniam, U. and Bhaskar, M.S.: Robust Queen Bee Assisted Genetic Algorithm (QBGA) Optimized Fractional Order PID (FOPID) Controller for Not Necessarily Minimum Phase Power Converters, IEEE Access, Vol. 9, pp. 93331–93337, 2021.

[22] Omar, A.I. Abdel Aleem, S.H.E. El-Zahab, E.E.A. Algablawy, M. and Ali, Z.M.: An improved approach for robust control of dynamic voltage restorer and power quality enhancement using grasshopper optimization algorithm, ISA Trans., Vol. 95, pp. 110–129, 2019.

[23] Abe, A.: Non-linear control technique of a pendulum via cable length manipulation: Application of particle swarm optimization to controller design, FME Trans., Vol. 41, No. 4, pp. 265–270, 2013.

[24] Pano, V. and Ouyang, P.R.: Gain tuning of position domain PID control using particle swarm optimization, Robotica, Vol. 34, No. 6, pp. 1351–1366, 2016.

[25] Wang, X. Shi, Y. Yan, Y. and Gu, X.: Intelligent welding robot path optimization based on discrete elite PSO, Soft Comput., Vol. 21, No. 20, pp. 5869–5881, 2017.

[26] Toha, S.F. Latiff, I.A. Mohamad, M. and Tokhi, M.O.: Parametric Modelling of a TRMS Using Dynamic Spread Factor Particle Swarm Optimisation, in: *11th International Conference on Computer Modelling and Simulation*, pp. 95–100, 2009.

[27] Xu, J.X. Guo, Z.Q. and Lee, T.H.: Design and implementation of integral sliding-mode control on an underactuated two-wheeled mobile robot, IEEE Trans. Ind. Electron., Vol. 61, No. 7, pp. 3671–3681, 2014.

NOMENCLATURE

δ_1 and δ_2	Acceleration coefficients
p_b	Best individual position of the current epoch, i
G_b	Best position in the population of the current epoch, i
$U(s)_{\text{FOPID}}$	Control signal of the FOPID control
α	Deviation of the particles in the search space
$e(t)$	Error between the desired height position response, $y_d(t)$ and the height position response of the system, $y_a(t)$
$E(s)$	Error in the s-domain
e	Exponential function
Ω	Inertia weight
i_{max}	Maximum number of epochs
MSE	Mean square error
p_n^{i+1}	New position
v_n^{i+1}	New velocity
PO	Percentage of overshoot
UDP	Percentage of undershooting
p^i_n	Position of the current epoch, i
$T_r(s)$	Rise time
$T_s(s)$	Settling time
ε	Spread of the particles in the search space
S_F	Spreading factor
e_{ss}	Steady-state error
N	Total number of sampling data
v_n^i	Velocity of the current epoch, u

ABBREVIATIONS

3D	Three-Dimensional
C1	Clamper 1
C2	Clamper 1
DC	Direct Current
FOPID	Fractional Order PID
MAVeP	Motorised Adjustable Vertical Platform
MS	Main Scissor
PID	Proportional-Integral-Derivative
PSO	Particle Swarm Optimisation
PSO-FOPID	FOPID Controller Tuned Using the PSO-SF Algorithm
PSO-SF	PSO with Spreading Factor
SS	Small Scissor
UP	Upper Deck

ДИЗАЈН, СИМУЛАЦИЈА И ЕКСПЕРИ–МЕНТАЛНО ИСПИТИВАЊЕ PSO-FOPID КОНТРОЛОРА ВИСИНЕ ПОЗИЦИЈЕ ПЛАТ–ФОРМЕ СА МЕХАНИЗМОМ МАКАЗА

Н.М.Х. Норсапери, С. Ахмад, С.Ф. Тоха, М.А. Абд Муталиб

Овај рад предлаже PSO-FOPID контролер, који је контролер фракционог реда пропорционално-интег–рално-деривативни (ФОПИД) подешен коришћењем оптимизације роја честица са алгоритмом фактора ширења за контролу положаја висине платформе механизма маказа. Процес подешавања пет конт–ролних појачања у ФОПИД контролеру представља технички изазов за постизање високе прецизности положаја. У овој студији је проблем обрађен методом ванмрежног подешавања коришћењем оп–тимизације роја честица са алгоритмом фактора ширења како би се смањила сложеност подешавања појачања контроле. Из експерименталне студије је откривено да предложени контролер може елими–нисати грешку устаљеног стања под две улазне референце са приближно 1,5% и 0,9% смањењем прекорачења и поднижења у одговору положаја висине у поређењу са његовим обећавајућим пер–

формансама у симулацијама. Потврђено је да PSO-FOPID контролер може бити користан у про–јектовању ефективне контроле положаја висине нелинеарне платформе.